Cyclic GMP Kinase I Modulates Glucagon Release From Pancreatic α-Cells

Veronika Leiss,[1,2] Andreas Friebe,[3] Andrea Welling,[1,4] Franz Hofmann,[1] and Robert Lukowski[1,5]

OBJECTIVE—The physiologic significance of the nitric oxide (NO)/cGMP signaling pathway in islets is unclear. We hypothesized that cGMP-dependent protein kinase type I (cGKI) is directly involved in the secretion of islet hormones and glucose homeostasis.

RESEARCH DESIGN AND METHODS—Gene-targeted mice that lack cGKI in islets (conventional cGKI mutants and cGKIα and Iβ rescue mice [α/βRM] that express cGKI only in smooth muscle) were studied in comparison to control (CTR) mice. cGKI expression was mapped in the endocrine pancreas by Western blot, immuno-histochemistry, and islet-specific recombination analysis. Insulin, glucagon secretion, and cytosolic Ca^{2+} ($[Ca^{2+}]_i$) were assayed by radioimmunoassay and FURA-2 measurements, respectively. Serum levels of islet hormones were analyzed at fasting and upon glucose challenge (2 g/kg) in vivo.

RESULTS—Immunohistochemistry showed that cGKI is present in α- but not in β-cells in islets of Langerhans. Mice that lack α-cell cGKI had significantly elevated fasting glucose and glucagon levels, whereas serum insulin levels were unchanged. High glucose concentrations strongly suppressed the glucagon release in CTR mice, but had only a moderate effect on islets that lacked cGKI. 8-Br-cGMP reduced stimulated $[Ca^{2+}]_i$ levels and glucagon release rates of CTR islets at 0.5 mmol/l glucose, but was without effect on $[Ca^{2+}]_i$ or hormone release in cGKI-deficient islets.

CONCLUSIONS—We propose that cGKI modulates glucagon release by suppression of $[Ca^{2+}]_i$ in α-cells. ***Diabetes*** **60: 148–156, 2011**

The complex and tightly controlled process of glucagon secretion from pancreatic α-cells is important for the maintenance of blood glucose homeostasis (1). Glucagon release is physiologically regulated by multiple signaling pathways that include neuronal control of α-cell function, paracrine factors such as insulin (2,3), and/or γ-aminobutyric acid (GABA) (4) released from β-cells, somatostatin (SST) secreted from adjacent δ-cells (5), and the inhibitory role of high blood glucose itself that directly acts on α-cells to suppresses glucagon release (3,6).

Controversial data have been reported for the physiologic significance of the nitric oxide (NO) pathway for islet functions. Both types of constitutive NOS (eNOS, nNOS) isozymes have been identified in islets (7–11). It was suggested that NO stimulates glucose-induced insulin release (7,10), was a negative modulator of insulin release (8,12,13) or had no effect (14). These discrepant results are probably caused by the analysis of various β-cell–derived cell lines compared with intact islets, the use of different types and concentrations of NO-donors and NOS-inhibitors. Additional data suggested that iNOS-derived NO is involved in autoimmune reactions that cause β-cell–dysfunction leading to insulin-dependent diabetes (15,16).

It has been difficult to discriminate between a direct action of NO on α-cells and an indirect effect of NO via β-cells since β-cell factors are potent inhibitors of α-cell activity (12,17,18). An important target of NO is the soluble guanylyl cyclase (sGC) that generates the second messenger cyclic guanosine-3′-5′-monophosphate (cGMP) (19). Some studies detected increased islet cGMP levels upon treatment with cytokines and L-arginine (12,15,20). cGMP analogues were reported to potentiate insulin release directly (21), suggesting that cGMP-dependent effectors are involved in the control of islet activity. The cGMP-dependent protein kinase type I (cGKI) is an important intracellular mediator of NO/cGMP signaling in many cells (22). The analysis of cGKI-deficient mice revealed that cGKI mediates the inhibitory effects of NO on platelet aggregation, the negative inotropic effect of NO/cGMP in the murine heart, and the NO-induced relaxation of blood vessels (22). However, cGKI knockout mice could not be analyzed reliably for a distorted islet function because they display abnormalities of various organ systems and die within the first 6 weeks (23). Recently, we generated an improved mouse model to study the specific roles of cGKI in vivo (24,25). These mice express either the cGKIα or cGKIβ isozyme selectively in smooth muscle cells (SMCs) on a cGKI-deficient genetic background. Since the animals show a prolonged life expectancy and normal SMC functions they were termed cGKIα and cGKIβ rescue mice (αRM and βRM, respectively).

We examined the role of cGKI for the regulation of glucose homeostasis using cGKI-KO mice (23) and rescue mice (RM) (24,25) models. We show that cGKI is expressed in the α-cells of the endocrine pancreas, whereas in different gene-targeted animals the cGKI protein was not detectable. Furthermore, we demonstrate that islet cGKI regulates glucagon release by modulation of the glucose-dependent changes of $[Ca^{2+}]_i$ that trigger exocytosis. These ex-vivo findings were supported by elevated serum levels of basal glucose and glucagon in intact RM animals.

From the [1]FOR 923, Technische Universität München, München, Germany, and Center for Integrated Protein Science, Ludwig-Maximilians-Universität München, München, Germany; [2]Institut für Pharmakologie und Toxikologie, Abteilung Pharmakologie und Experimentelle Therapie, Universitätsklinikum Tübingen, Tübingen, Germany; [3]Lehrstuhl für Physiologie I, Julius-Maximilians Universität Würzburg, Würzburg, Germany; [4]Institut für Pharmakologie und Toxikologie, Technische Universität München, München, Germany; and [5]Institut für Pharmazie, Abteilung Pharmakologie, Toxikologie und Klinische Pharmazie, Universität Tübingen, Tübingen, Germany.

Corresponding author: Robert Lukowski, robert.lukowski@uni-tuebingen.de.

Received 27 April 2010 and accepted 7 October 2010. Published ahead of print at http://diabetes.diabetesjournals.org on 26 October 2010. DOI: 10.2337/db10-0595.

RESEARCH DESIGN AND METHODS

Experimental animals. The generation of the conventional cGKI-knockout mice (cGKI-KO; genotype: $cGKI^{L-/L-}$) (23) and cGKIα and Iβ rescue animals (αRM; genotype: $SM22\alpha^{+/I\alpha}$; $cGKI^{L-/L-}$ and βRM; genotype: $SM22\alpha^{+/I\beta}$; $cGKI^{L-/L-}$) has been described (25). All animals were maintained and bred in the animal facility of the Institut für Pharmakologie und Toxikologie, Technische Universität München and had free access to water and standard chow. The experimental procedures were approved by the local government's Committee on Animal Care and Welfare in Oberbayern. For in vivo experiments, male gene-targeted cGKI animals were used and compared with their age and littermate controls on a 129Sv inbred background (CTR; genotype: $cGKI^{+/L-}$ and/or $cGKI^{+/+}$). The GLUC-Cre mouse (26) and the RIP-Cre mouse (27) were crossed to mice that carry loxP-flanked cGKI alleles (L2) (28) to generate cGKI mutants with recombined cGKI-null alleles (L−) in α or β-cells, respectively. The tissue-specific cGKI knockouts on a C57/BL6N genetic background were termed "α-cell cGKI knockout" ($cGKI^{acko}$; genotype: GLUC-$Cre^{tg/+}$; $cGKI^{L-/L2}$) and "β-cell cGKI knockout" ($cGKI^{bcko}$, genotype: RIP-$Cre^{tg/+}$; $cGKI^{L-/L2}$). For experiments the $cGKI^{acko}$ and $cGKI^{bcko}$ mice were compared with littermate controls (genotype: GLUC-$Cre^{tg/+}$; $cGKI^{+/L2}$ and RIP-$Cre^{tg/+}$; $cGKI^{+/L2}$). The R26-stop-eYFP reporter mice were from the Jackson Laboratory strain# 006148. Upon Cre-mediated excision of an intervening stop sequence, eYFP was expressed in α-cells of GLUC-$Cre^{tg/+}$; $eYFP^{tg/+}$ mice.

Determination of body fat. We compared 5- to 6-week-old cGKI-KO mice and 15- to 20-week-old αRM mice with their littermate controls. Mice were killed by cervical dislocation and weighed (wet weight). The water fraction was extracted by incubation of the bodies at 90°C for 24 h. The dried mummies were weighed (dry weight), homogenized, and then transferred to an extraction sleeve. The body fat was extracted by chloroform used as a organic solvent in a soxhlet apparatus After five extraction cycles, the nonsoluble portion remained in the sleeve and the extracted fat was collected in the chloroform. The sleeves were dried for 12 h at 90°C and weighed again. The body fat content was the weight difference of the mummified bodies before and after the soxhlet extraction.

Serum hormone determinations. The 96-well fluorescent LINCOplex microplate immunoassay (Millipore) was used to determine simultaneously the concentrations of glucagon and insulin in 10 μl mouse serum in the presence of dipeptidyl peptidase IV inhibitors and aprotinin. A combination of fluorescent beads that bind to glucagon or insulin-specific antibodies and biotinylated detection antibodies allow for a specific quantification of the islet hormones. The assay was performed according to the manufacturers' recommendations and then quantified in a Bio-Plex micro-plate reader.

Isolation of islets. Islets were isolated according to previous studies (29). In brief, islets were isolated by the retrograde injection of a digestion solution (1.9 units/ml collagenase/HBSS; Sigma Aldrich) into the pancreas. Islets were purified by several washings, picked by hand, and transferred to culture medium (RPMI-1640, 5 mmol/l glucose, 100 units/ml penicillin, 100 μg/ml streptomycin, 10% FCS). The protein/RNA extractions were performed on pooled islets isolated from 3 to 6 animals.

Western blot analysis. Overnight-cultured islets were thoroughly rinsed by three changes of PBS and then homogenized in 50 μl protein lysis buffer (20 mmol/l Tris-HCl, pH 8.3; 0.67% SDS; 238 mmol/l β-mercaptoethanol; 0.2 mmol/l PMSF). Proteins obtained from 100 islets were separated on 8% SDS-polyacrylamide gels. Immunodetection was performed by using the primary antibodies specific for cGKI common (30) (dilution 1:200), cGKIα (30) (dilution 1:500), cGKIβ (30) (dilution 1:500), β-actin (Abcam) (dilution 1:10,000), PDE-5 (24) (dilution 1:500), inositol 1,4,5,-triphosphate receptor associated cGMP kinase substrate (IRAG) (30) (dilution 1:300), or somatostatin (Santa-Cruz) (dilution 1:2,000).

Immunohistochemistry and fluorescence. Immunodetection was performed on paraffin-embedded serial 8- to 10-μm sections of the pancreas as previously published (24). Biotinylated secondary antibodies (1:200 dilution; Vector Laboratories) in combination with the avidin-biotin method (Vector Laboratories) were used to identify primary antibody/antigen complexes by immunohistochemistry. Visualization of the immune complexes was carried out by Vector Blue substrate (Vector Laboratories) or diaminobenzidine (brown staining) (Sigma-Aldrich).

Alternatively, primary antibody/antigen complexes were detected with secondary antibodies conjugated to fluorescent dyes (1:200 dilution, Dianova), and then the fluorescence signals were visualized by a confocal laser scanning microscope (LSM510, Zeiss). Primary antibodies used were specific for cGKI (1:50 dilution) (30), cGKIα (1:50 dilution) (30), insulin (1:2,500 dilution; DAKO), glucagon (1:2,000 dilution, Sigma-Aldrich), somatostatin (1:1,000 dilution, Santa-Cruz), and $sGC\beta_1$ (1:200 dilution) (19).

Islet/striated muscle RNA isolation for RT-PCR analysis. After 18–24 h in culture, islets were thoroughly rinsed by three changes of PBS, transferred to RNAse-free reaction tubes, and shock frozen in liquid nitrogen. RNA was extracted by the peqGOLD RNA pure reagent (PEQLab). 500 μl peqGOLD reagent was used for the purification of total RNA from 500 islets.

Skeletal muscles from murine hind limbs were used for RT-PCR analysis. The purified RNA was dissolved in 50 μl diethyl-pyrocarbonate treated ddH_2O, quantified by standard ultraviolet photometry, and stored at −20°C until RT-PCR was carried out. The mRNA transcripts coding for cGKIα, $sGC\alpha_2$, $sGC\beta_1$, Npr-1 (GC-A), Npr-2 (GC-B), and GLUT4 in islets/striated muscles were standardized to the mRNA of hypoxanthine phosphoribosyltransferase (HRPT) coamplified in the same reaction. The primer sequences and the size of the fragments amplified were: cGKIα (425 bp) forward 5′-GGAAGTTCAC TAAATCCGAGAG-3′, reverse 5′-TGAGGATTTCATCAGGAAGG-3′; $sGC\alpha_2$ (303 bp) forward 5′-AGATGCTCCTATGCAGACC-3′, reverse 5′-CATCAGAG TACCTTCAGGAAGC-3′; $sGC\beta_1$ (251 bp) forward 5′-AGCCCTTACACCTT; CTGC-3′, reverse 5′-CACTCAAGTTTCTCCACATCC-3′; Npr-1 (357 bp) forward 5′-AGGCGCTTGTGCTCTATG-3′, reverse 5′-TATCCTGCCCATCGTCTC-3′; Npr-2 (364 bp) forward 5′-AGCCATGCCCTCTATGC-3′, reverse 5′-ATATG CTGGTACCACCTTCC-3′; GLUT4 (381 bp) forward 5′-TCGTCATTGGCAT TCTGGT-3′, reverse 5′-CATTGATGCCTGAGAGCTGTT-3′; HPRT (175 bp) forward 5′-GTAATGATCAGTCAACGGGGGAC-3′, reverse 5′-TGGTTAAGGTTG CAA GCTTGCTGG-3′.

Ex-vivo islet glucagon/insulin release. Freshly isolated islets were preincubated for 30 min at 37°C in a Krebs-Ringer buffer (KRB) at pH 7.4 containing in mmol/l: 120 NaCl, 25 $NaHCO_3$, 4.7 KCl, 1.2 $MgSO_4$, 2.5 $CaCl_2$, 1.2 KH_2PO_4, 5 glucose, 10 HEPES and 1 mg/ml BSA. Groups of 10 and 20 islets were incubated for 60 min at 37°C in 200-μl KRB buffer for the determination of insulin or glucagon, respectively.

Ca^{2+} imaging. Freshly isolated islets were incubated in a humidified incubator for 4 h. Islets were loaded with 10 μmol/l Fura-2AM (Calbiochem) in KRB buffer at 37°C for 30 min. Thereafter, islets were washed and then perfused with bath solution at 1 ml/min at 37°C in a chamber on the microscope stage. Experiments were performed using a Zeiss microscope with a Zeiss Fluor 205 40× objective and a cooled charge-coupled device camera. Dual excitation at 340/380 nm was used and emission at 510 nm measured (TILLviSION software, Till Photonics, Gräfelfing, Germany). Every 700 ms, 20 ms exposures were taken. The frequency of changes in the $[Ca^{2+}]_i$ oscillations and the peak amplitudes were determined and normalized to the 340/380 nm ratios. Only cells displaying a distinct response to 5 and 0.5 mmol/l glucose or 20 mmol/l glucose were included in these calculations.

RESULTS

Basal glucose homeostasis in cGKI gene-targeted mice. To investigate whether physiologic glucose homeostasis in the intact animal depends on the presence of cGKI, we used three gene-targeted models of cGKI deficiency, i.e., conventional cGKI knockout mice (cGKI-KO) that do not express the cGKI isozymes in any cell (23) and mice that express either the cGKIα or cGKIβ (αRM and βRM, respectively) isozyme under the control of the endogenous SM22α promoter specifically in SMCs on a cGKI-deficient background (24,25). Serum glucose concentrations were significantly higher after 12-h fasting in the cGKI-KO (Fig. 1*A*), αRM (Fig. 1*B*), and βRM than in the CTR mice. Fasting blood glucose levels were 45.5 ± 1.5 mg/dl (n = 12) in 6- to 8- week-old CTR mice, 61.4 ± 2.9 mg/dl (n = 9) in 6- to 8-week-old cGKI-KO mice, 71.8 ± 2.3 mg/dl (n = 18) in 15- to 20-week-old βRM mice, 90.7 ± 3.2 mg/dl (n = 26) in 15- to 20-week-old αRM mice, and 57.4 ± 1.3 mg/dl (n = 53) in age-matched CTR mice. Since these results suggested that αRM and βRM mice had an identical hyperglycemic phenotype, we used αRM mice for further experiments. The glucagon serum concentrations were significantly elevated in αRM (22.3 ± 3.6 pmol/l; n = 8) compared with CTR mice (CTR 15.2 ± 1.8 pmol/l; n = 21) (Fig. 1*C*). Interestingly, basal serum insulin levels did not differ between the two genotypes (Fig. 1*D*). These findings suggest that cGKI is involved in the control of glucose homeostasis at fasting.

In vivo glucose and insulin tolerance. We performed insulin and oral glucose tolerance test (OGTT) to examine whether the elevated glucose and glucagon levels in the

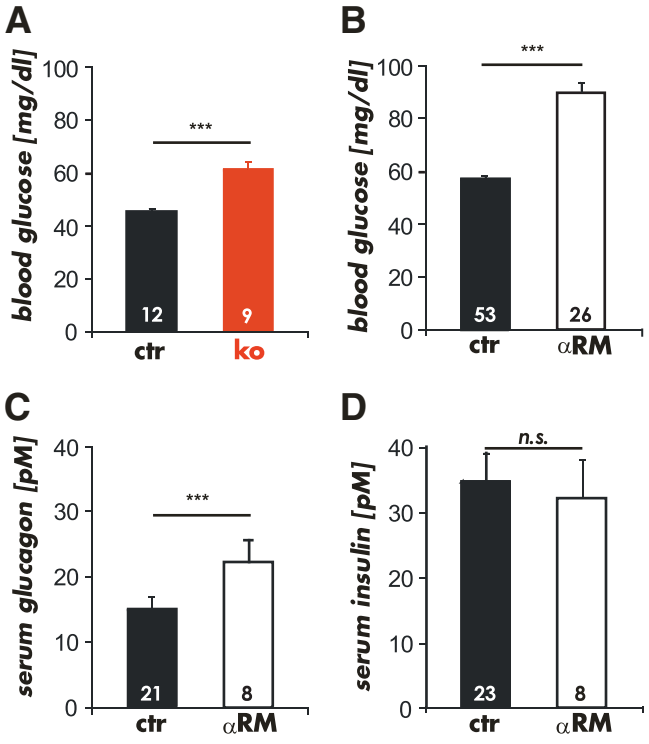

FIG. 1. Basal blood glucose and serum hormone levels of mice lacking cGKI in islets after 12-h fasting. *A*: Basal blood glucose levels determined from 6- to 8-week-old cGKI-KO (ko) mice and their littermate controls (ctr). *B*: Basal blood glucose levels measured in 15- to 30-week-old αRM and control (ctr) mice. *C*: The average serum glucagon levels of fasted αRM were significantly increased in comparison with CTRs. *D*: The analysis of serum insulin revealed no differences between αRM compared with littermate controls (*$P < 0.001$). (A high-quality color representation of this figure is available in the online issue.)**

fasted state reflected an altered glycemic control of gene-targeted mice. We induced hypoglycemia by intraperitoneal injection of insulin. Blood glucose levels were monitored during 180 min in 12-h fasted αRM and CTR mice. Within 60 min, insulin lowered the blood glucose to the same minimal level (supplementary Fig. 1 in the online appendix available at http://diabetes.diabetesjournals.org/cgi/content/full/db10-0595/DC1.). Both types of mice were able to counter-regulate the blood glucose levels to physiologic levels within 180 min (supplementary Fig. 1). These data suggest that glucose handling after a single high dose of exogenous insulin was not disturbed in αRM animals.

In contrast, the OGTT was significantly improved in αRM animals as compared with CTR littermates (supplementary Fig. 2*A*). During the first 15 min, blood glucose levels increased in CTR and αRM animals. Blood glucose levels continued to increase in CTR animals, whereas they remained constant in αRM mice at 30 min, indicating a faster glucose clearance. Thereafter, blood glucose level decreased in both animal types and reached 223.7 ± 18.3 mg/dl; $n = 15$ and 143 ± 20.2 mg/dl; $n = 11$ after 60 min in CTR and αRM mice, respectively. No differences were detectable between both genotypes at 120 min.

During the entire OGTT, αRM animals had higher glucagon levels than CTR mice (supplementary Fig. 2*B*). Values were significantly higher at 5 min (CTR 13.3 ± 1.6 pmol/l; $n = 8$; αRM 20.8 ± 1.8 pmol/l; $n = 8$), 15 min (CTR 11.6 ± 2.3 pmol/l; $n = 5$; αRM 18.9 ± 1.7 pmol/l; $n = 8$), 30 min (CTR 14.9 ± 3.4 pmol/l $n = 6$; αRM 17.6 ± 1.5 pmol/l $n = 7$), and 120 min (CTR 12.9 ± 2.4 pmol/l $n = 7$; αRM 18.6 ± 2.2 pmol/l $n = 8$).

In the presence of higher glucose levels (see Fig. 1) basal insulin levels did not differ between CTR and αRM mice (supplementary Fig. 2*C*). However, 15 min after glucose application, serum insulin concentration was higher in αRM than in CTR animals (CTR 68.5 ± 12.2 pmol/l; $n = 11$; αRM 84 ± 19 pmol/l; $n = 8$), but these values did not reach statistical significance.

Since the superior glucose tolerance of αRM mice was not based on an improved glucose-stimulated response of pancreatic β-cells to secrete insulin, we hypothesized that it must be due to enhanced peripheral insulin sensitivity. It is known that the gene-targeted cGKI mice weigh less than their littermate CTRs. Therefore, we tested if the improved clearance of glucose from the serum was responsible for the altered OGTT profile. The total body fat mass and serum lipids were significantly lower in cGKI-KO and αRM mice as compared with littermate CTRs (supplementary Fig. 2*D–F*). In addition, we found higher levels of the insulin-dependent glucose transporter 4 (GLUT4) mRNA in striated muscle preparations (supplementary Fig. 2*G*). These results implicate that the OGTT of gene-targeted cGKI mice was improved indirectly by changes in the body periphery.

Expression analysis of islet cGKI. Since glucagon secretion was deregulated in cGKI mutant mice, we hypothesized that cGKI may be expressed in the islets. Western blots identified the cGKI protein in islets of CTR mice, whereas no cGKI protein was detectable in the islets of conventional cGKI-KOs, αRM, and βRM animals (Fig. 2*A*). As reported previously (25), the cGKI protein was present in the stomach of the αRM and βRM mice. In contrast, cGKI expression was not detectable in SMCs and other organ systems of the cGKI-KO mice (Fig. 2*B*).

Immunohistochemical analysis mainly identified cGKI in a subset of cells that localized to the mantle of the islets (Fig. 2*C*). As expected, small vessels containing SMCs were positively stained for cGKI in CTR, αRM, and βRM mice, but remained unstained in cGKI-KO animals (Fig. 2*C*). Islets of conventional cGKI-KOs, as well as islets of αRM and βRM mice were not stained for cGKI, confirming that they lack the cGKI protein (Fig. 2*C*). The cGKI-expressing cells were not stained by an insulin antibody (24,25,30), indicating that the two proteins were not coexpressed in β-cells (supplementary Fig. 3*A*). The insulin expression pattern of cGKI-deficient islets in cGKI-KO, αRM, and βRM animals was not different from the pattern of CTR islets (supplementary Fig. 3*A*). A subpopulation of δ-cells that were detected by the δ-cell marker SST showed colocalization of SST and cGKI (supplementary Fig. 3*B*). However, in most SST-positive cells, cGKI was absent. SST expression was not altered in the different cGKI-deficient islets (supplementary Fig. 3*B*). High-resolution immunofluorescence experiments clearly demonstrated colocalization of cGKI and glucagon in all α-cells (Fig. 3). Again, the cGKI protein was not detected in cGKI-deficient islets of cGKI-KO, αRM, and βRM mice, whereas the quantity and intensity of glucagon-stained cells was similar. The absence of the cGKI protein did not affect the size and the number of islets per pancreatic cross-section area, the amount of cells per islets, and their cellular combination (data not shown).

To support the observation that cGKI is expressed in α-but not in β-cells, we used the RIP-Cre mouse, which is able to generate efficient β-cell-specific inactivation of

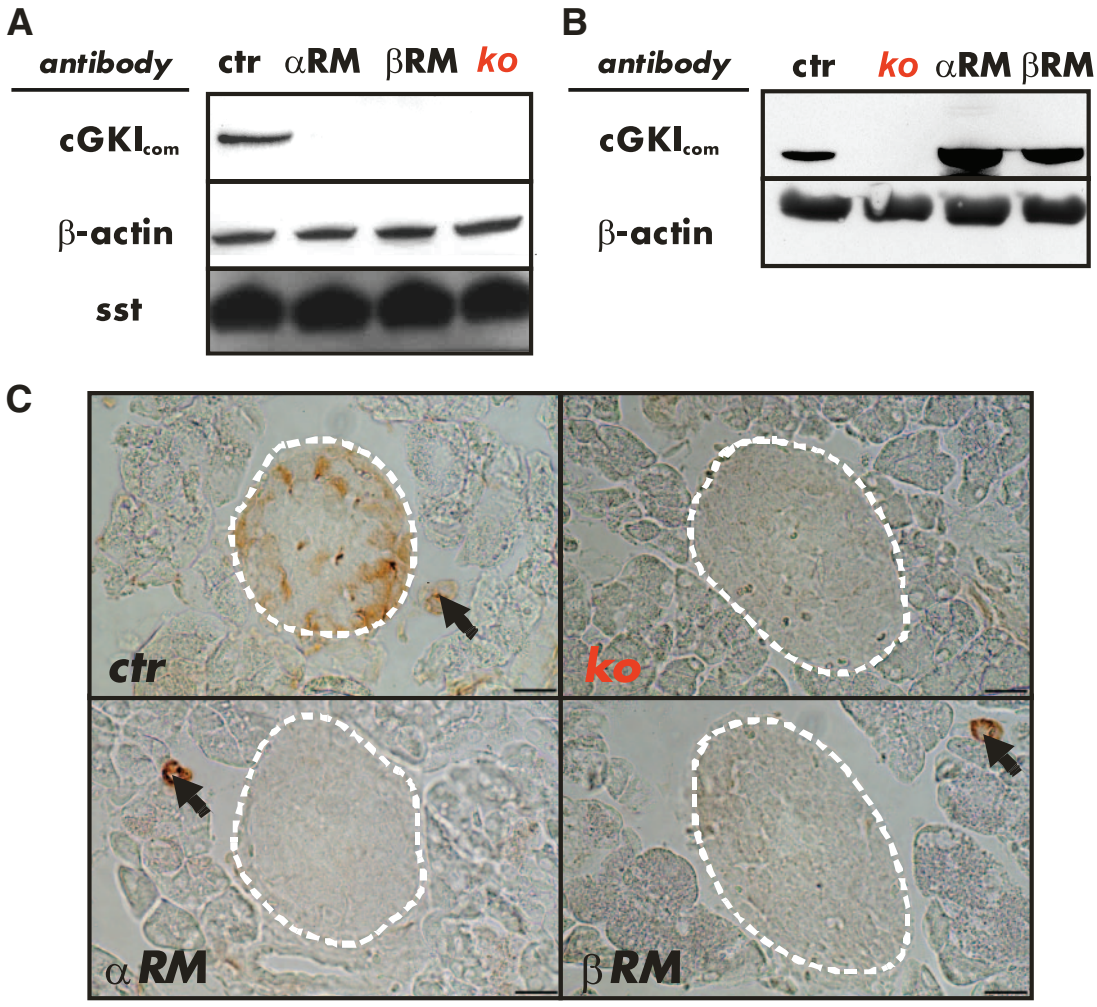

FIG. 2. cGKI is expression in pancreatic islets. ***A*****: The cGKI protein was present in islet lysates of control (CTR, genotype: cGKI$^{+/+}$ or cGKI$^{+/L-}$) islets but not detectable in islet homogenates from cGKI-KO (KO, genotype: cGKI$^{L-/L-}$), αRM (genotype: SM22α$^{+/Icre}$; cGKI$^{L-/L-}$) and βRM (genotype: SM22β$^{+/Iβ}$; cGKI$^{L-/L-}$) mice. A cGKI common antibody (cGKI$_{com}$) (30) was used to identify the respective protein. β-actin was used as loading control and somatostatin (sst) as a marker of pancreatic islets.** ***B*****: Western blot analysis demonstrating expression of the cGKI protein in the stomach of control (ctr), αRM, and βRM mice, but no expression in cGKI-KO (KO) mice. β-actin was used as loading control.** ***C*****: Immunohistochemical stainings of cGKI protein showing expression in control islets (*dotted line*) and smooth muscle cells (SMCs) of small blood vessels (*arrows*). Pancreatic sections from αRM and βRM animals show cGKI expression in the exocrine pancreas that was restricted to the vasculature (*arrows*), whereas the cGKI-KO pancreatic sections completely lacked the cGKI protein in both islets and SMCs. For better illustration, a *white dotted line* was added to indicate the islet's perimeter. Scale bar, 20 μm. (A high-quality color representation of this figure is available in the online issue.)**

floxed target genes (27). We crossed the RIP-Cre mice to a floxed cGKI mouse line (28) and generated the β-cell–specific cGKI-knockouts (cGKI^{bcko}). Expression of cGKI was unchanged in islets of cGKI^{bcko} mice, confirming that cGKI is not present in β-cells (supplementary Fig. 4*A*). Basal fasting glucose levels of cGKI^{bcko} mice were not different from their respective controls (supplementary Fig. 4*B*). Vice versa, we used the GLUC-Cre mouse expressing the Cre recombinase specifically in α-cells (26). Mating of the GLUC-Cre mice with the floxed cGKI animals generated α-cell cGKI knockouts (cGKI^{acko}). In comparison with age and littermate controls, no increase of the basal glucose was noted in cGKI^{acko} mice (supplementary Fig. 4*D*). We anticipated that the ablation of cGKI in α-cells was inadequate to produce hyperglycemia in vivo. Indeed, protein levels of islet cGKI in cGKI^{acko} were reduced but not depleted (supplementary Fig. 4*C*), probably because cGKI was still present in some α-cells, caused by *1*) a patchy recombination process, and *2*) the presence of cGKI in δ-cells (see supplementary Fig. 3*B* and *C*). Together these results indicate that cGKI is expressed in islet α-cells of the mouse and might therefore affect the synthesis or release of glucagon.

Analysis of cGKI isoforms, target proteins, and key components for cGMP synthesis. Two distinct isoforms of cGKI, Iα and Iβ, are present in different tissues. Western blot analysis of islet protein homogenates identified only the Iα protein in control islets (supplementary Fig. 5*A*). As expected, the cGKI protein was not detectable in the gene-targeted cGKI animals (supplementary Fig. 5*A*). In line with the absence of the cGKIβ isoform, the cGKIβ-specific target inositol 1,4,5-triphosphate receptor associated cGMP kinase substrate (IRAG) was not detectable in pancreatic islets, whereas the *cGMP*-specific phosphodiesterase-5 (PDE-5) was present in the same protein homogenates (supplementary Fig. 5*A*). These results excluded possible false-positive cGKI signals in the islet protein samples caused by a contamination with platelets or blood vessels, since both express mainly the cGKIβ isoform (30). In line with the immunoblot data (supplementary Fig. 5*A*),

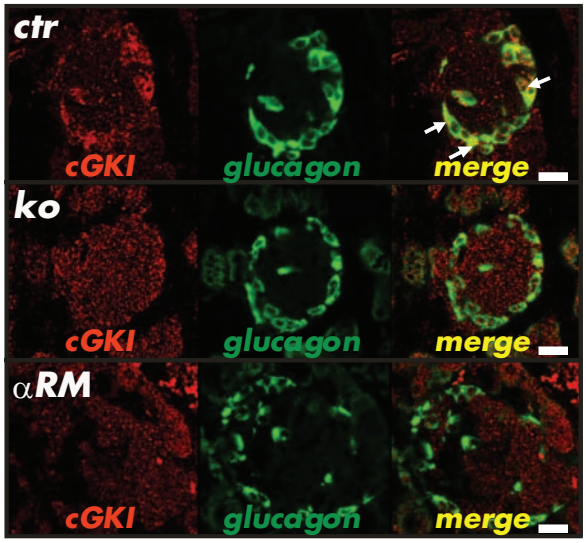

FIG. 3. Immunofluorescence analysis of cGKI and glucagon. Colocalization (*white arrows*) of glucagon (*green*) and cGKI (*red*) was detectable only in islets of control mice (*merge*). The glucagon signal in cGKI-KO (KO) and αRM animals was well detectable in the mantle of the islets, but no coexpression with the cGKI protein was found. Scale bar, 20 μm. (A high-quality color representation of this figure is available in the online issue.)

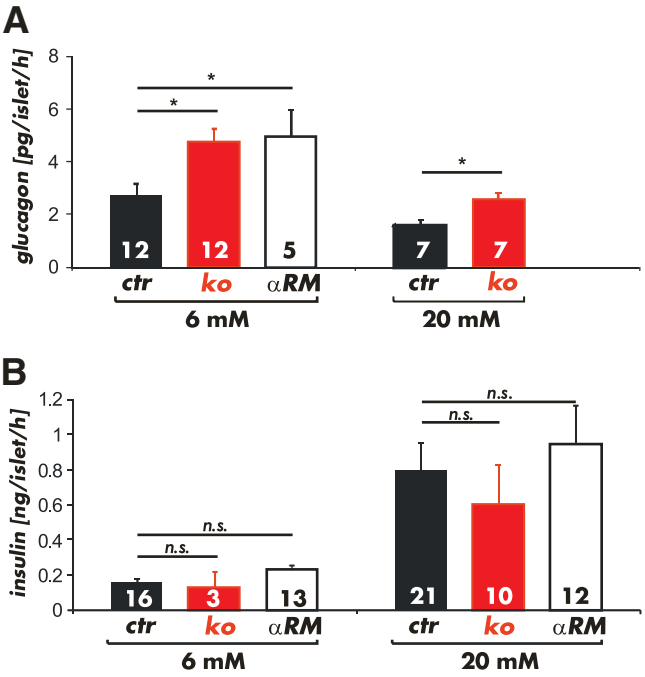

FIG. 4. Insulin and glucagon release from intact islets. *A*: Glucagon release from isolated cGKI-KO (KO) islets (*red bars*) and αRM islets (*open bars*) was increased at 6 mmol/l as compared with isolated control islets (*black bars*). Although control and cGKI-KO islets were able to decrease glucagon secretion at 20 mmol/l glucose, the glucagon release was yet significantly higher in cGKI-deficient (*red bars*) islets. (*$P < 0.05$). *B*: Insulin release from isolated cGKI-KO (KO) and αRM islets was unchanged at high (20 mmol/l) and basal (6 mmol/l) glucose concentrations compared with control (CTR) islets. (A high-quality color representation of this figure is available in the online issue.)

immuno-histochemical analysis with the cGKIα specific antibody and semiquantitative RT-PCR analysis using a cGKIα-specific primer pair confirmed that the cGKI positive cells (Fig. 2*C*) expressed the Iα isozyme (supplementary Fig. 5*B* and *C*).

In general, cGKI is activated by increased cGMP levels. Therefore, we analyzed the expression of soluble and particulate guanylyl cyclases (sGC and pGC, respectively) using cDNA templates generated from purified islet total RNA of control animals. We identified the transcripts for the natriuretic peptide receptor-1 (NPR-1/pGC-A) and NPR-2/pGC-B in islets (supplementary Fig. 6*A*). In addition, the β_1 and α_2 subunit of the sGC were expressed in islets, indicating that a functional NO-sensitive cyclase might be formed (supplementary Fig. 6*B*). Immunofluorescence analysis revealed that the catalytic β_1 subunit of the sGC specifically localized to the glucagon positive α-cells (supplementary Fig. 6*C*). These data suggest that cGMP accumulation and subsequent activation of cGKI in islets can be attained by both the NO/sGC and the NP/pGC pathways (31,32).

Ex vivo insulin/glucagon secretion. The results presented so far suggest that the gene-targeted cGKI mice lack cGKI in α-cells. The observed changes in glucagon secretion and glucose homeostasis might therefore be related to the absence of cGKI in islets. To test this hypothesis, we determined glucagon secretion in isolated islets. The mean total glucagon content was not different between CTR (2.82 ± 0.1 ng/islet; $n = 23$), cGKI-KO (3.1 ± 0.14 ng/islet; $n = 20$), and αRM (2.3 ± 0.8 ng/islet; $n = 21$) islets. The cGKI negative islets exposed to 6 mmol/l glucose released significantly more glucagon than CTR islets (CTR 2.7 ± 0.4 pg/islet/h; KO 4.7 ± 0.5 pg/islet/h, αRM 4.9 ± 0.5 pg/islet/h) (Fig. 4*A*). In our ex-vivo experiments, we did not notice maximal inhibition of glucagon release at moderate glucose concentrations (around 7 mmol/l) (33) since glucagon secretion from both CTR and cGKI-KO islets was further suppressed after exposure to 20 mmol/l glucose (1,3,6). In agreement with the data from intact animals (see Fig. 1*C* and supplementary Fig. 2*B*), the total glucagon release rates from cGKI negative islets were still higher (CTR 1.6 ± 0.2 pg/islet/h; [$n = 7$] vs. KO 2.6 ± 0.2 pg/islet/h [$n = 7$]) (Fig. 4*A*).

In line with the in vivo data (see Fig. 1*D* and supplementary Fig. 2*C*), no differences could be found for the release of insulin using isolated islets from all three genotypes. Release rates were similar at 6 mmol/l glucose (CTR 0.15 ± 0.02 ng/islet/h; KO 0.13 ± 0.09 ng/islet/h, αRM 0.22 ± 0.03 ng/islet/h) and significantly increased to comparable levels upon exposure of the islets to 20 mmol/l glucose (CTR 0.8 ± 0.1 ng/islet/h; KO 0.6 ± 0.2 ng/islet/h, αRM 0.9 ± 0.2 ng/islet/h). The total insulin content of the islets (in μg/islet) was similar for CTR (0.35 ± 0.03 ($n = 15$)) and αRM (0.38 ± 0.2 ($n = 21$) mice. Taken together, the ex-vivo hormone secretion experiments demonstrated that the deletion of cGKI in pancreatic islet cells increased glucagon releasing rates even at 20 mmol/l glucose.

$[Ca^{2+}]_i$ measurements of isolated islets. It is generally accepted that glucagon release is linked to an increase in $[Ca^{2+}]_i$ (1,34). As recognized for many physiologic processes, such as vascular tone, platelet activation, and synaptic plasticity (22), we hypothesized that cGKI might interfere with the rise of $[Ca^{2+}]_i$, that triggers glucagon secretion in α-cells. We used genetically-labeled α-cells that expressed the yellow fluorescent protein (eYFP) (35) to characterize $[Ca^{2+}]_i$ signals of individual cells in response to glucose changes (supplementary Fig. 7*A*). Changes in $[Ca^{2+}]_i$ were monitored in FURA-2 loaded individual islet cells. As expected, glucose-responsive β-cells were inactive at low glucose (0.5–5 mmol/l), but showed an increase in $[Ca^{2+}]_i$ oscillations at 20 mmol/l. In

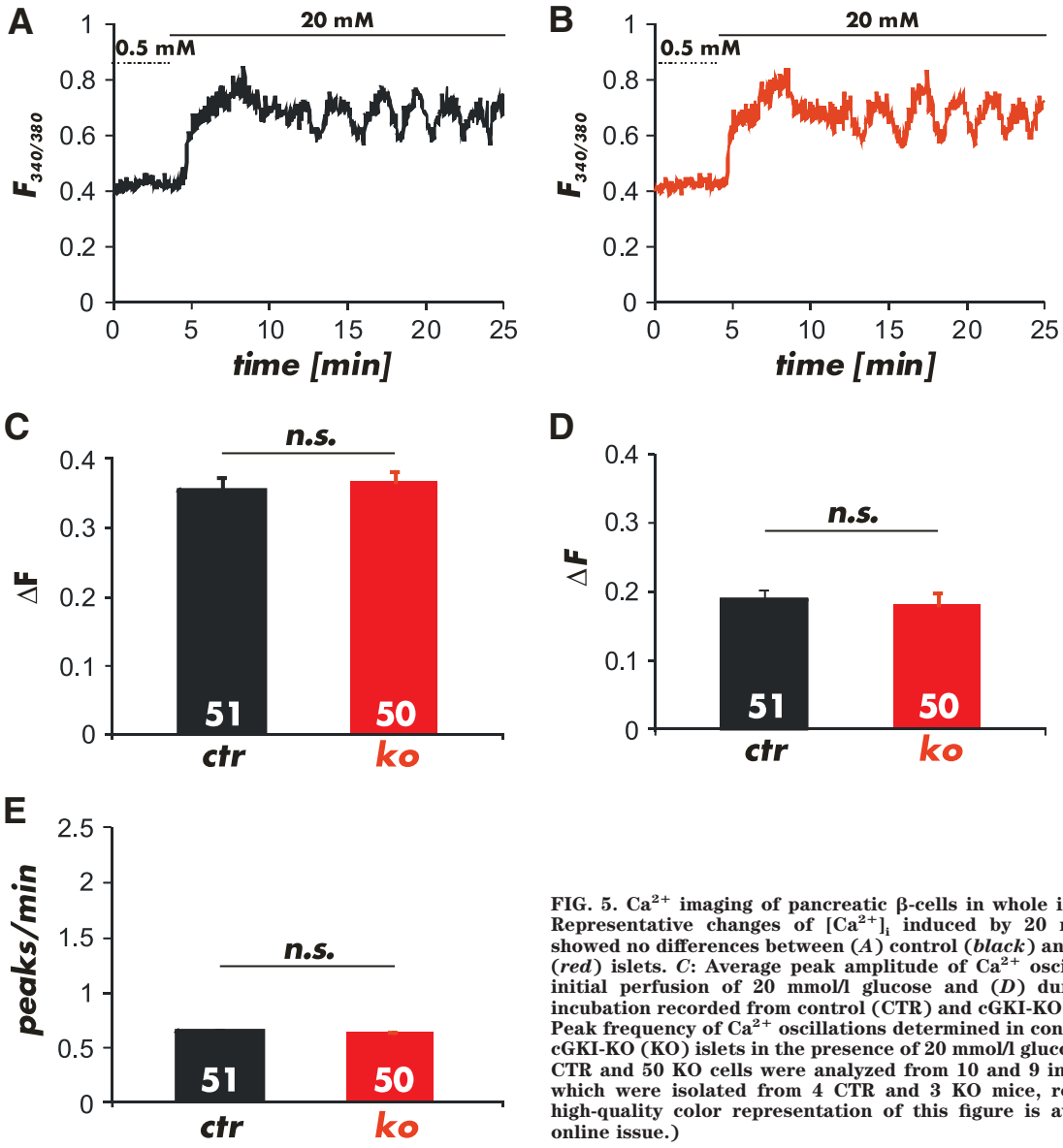

FIG. 5. Ca^{2+} imaging of pancreatic β-cells in whole islets. *A* and *B*: Representative changes of $[Ca^{2+}]_i$ induced by 20 mmol/l glucose showed no differences between (*A*) control (*black*) and (*B*) cGKI-KO (*red*) islets. *C*: Average peak amplitude of Ca^{2+} oscillations at the initial perfusion of 20 mmol/l glucose and (*D*) during prolonged incubation recorded from control (CTR) and cGKI-KO (KO) islets. *E*: Peak frequency of Ca^{2+} oscillations determined in control (CTR) and cGKI-KO (KO) islets in the presence of 20 mmol/l glucose. In total, 51 CTR and 50 KO cells were analyzed from 10 and 9 individual islets, which were isolated from 4 CTR and 3 KO mice, respectively. (A high-quality color representation of this figure is available in the online issue.)

contrast, the eYFP-positive cells showed an increased amplitude and frequency of $[Ca^{2+}]_i$ at 5 and 0.5 mmol/l, whereas $[Ca^{2+}]_i$ transients were suppressed at 20 mmol/l glucose (supplementary Fig. 7*B*) as described earlier for α-cells (1,36). For subsequent experiments, we therefore used 0.5, 5, and 20 mmol/l glucose, since these concentrations allow discriminating between α- and β-cells. It was reported that single α-cells in culture do not respond adequately to glucose when paracrine effects of β-cells are absent (37,38). We therefore performed further analysis of $[Ca^{2+}]_i$ transients in intact islets, which we considered to be more physiologic. All values are given as fluorescence ratio of FURA-2 at 340/380 nm and difference of 2 FURA ratio values (ΔF).

An increase in glucose from 0.5 to 20 mmol/l induced a significant elevation in $[Ca^{2+}]_i$ in CTR and cGKI-KO islets (Fig. 5*A* and *B*). The ratio of the FURA-2 values for the amplitude of the first Ca^{2+}-peak (CTR 0.37 ± 0.02 n = 51; KO 0.35 ± 0.01 n = 50), of the oscillations (CTR 0.18 ± 0.02, n = 51; KO 0.17 ± 0.02; n = 50) (Fig. 5*C* and *D*) and the frequency of the $[Ca^{2+}]_i$ oscillations (CTR 0.66 ± 0.01 peaks/min; n = 51; KO 0.65 ± 0.02 peaks/min; n = 50) (Fig. 5*E*) at 20 mmol/l glucose were not different between CTR and cGKI-KO islets indicating that the β-cell response to the change in glucose concentration did not differ between the genotypes. At 0.5 and 5 mmol/l glucose (Fig. 6*A* and *B*), concentrations at which only changes of $[Ca^{2+}]_i$ in α-cells were observed (see supplementary Fig. 7*B* and *C*), the oscillation frequency of Ca^{2+}-peaks was increased in cGKI-KO compared with CTR islets (CTR 1.1 ± 0.05 peaks/min; n = 68, and 0.8 ± 0.05 peaks/min; n = 68; KO 1.8 ± 0.06 peaks/min; n = 67 and 2.2 ± 0.05 peaks/min; n = 67) (Fig. 6*E*). These values were significant different at $P < 0.001$. Preincubation of islets with 8-Br-cGMP (1 mmol/l), a membrane-permeable analog of cGMP, reduced the oscillation frequency of the Ca^{2+}-peaks at 0.5 mmol/l glucose to 0.01 ± 0.01 peaks/min (n = 30) in CTR α-cells, whereas 8-Br-cGMP had no effect in cGKI-KO islets (2.11 ± 0.04 peaks/min; n = 47) (Fig. 6*C–E*). Furthermore, we noticed a significant increase in the frequency of $[Ca^{2+}]_i$ oscillations in α-cells of cGKI-KOs at all glucose concentrations tested (Fig. 6*E*).

These experiments indicated that cGKI significantly affected the glucose-induced changes of the $[Ca^{2+}]_i$ oscillation of α-cells. They suggested that cGKI might also affect glucagon secretion in CTR α-cells if activated by

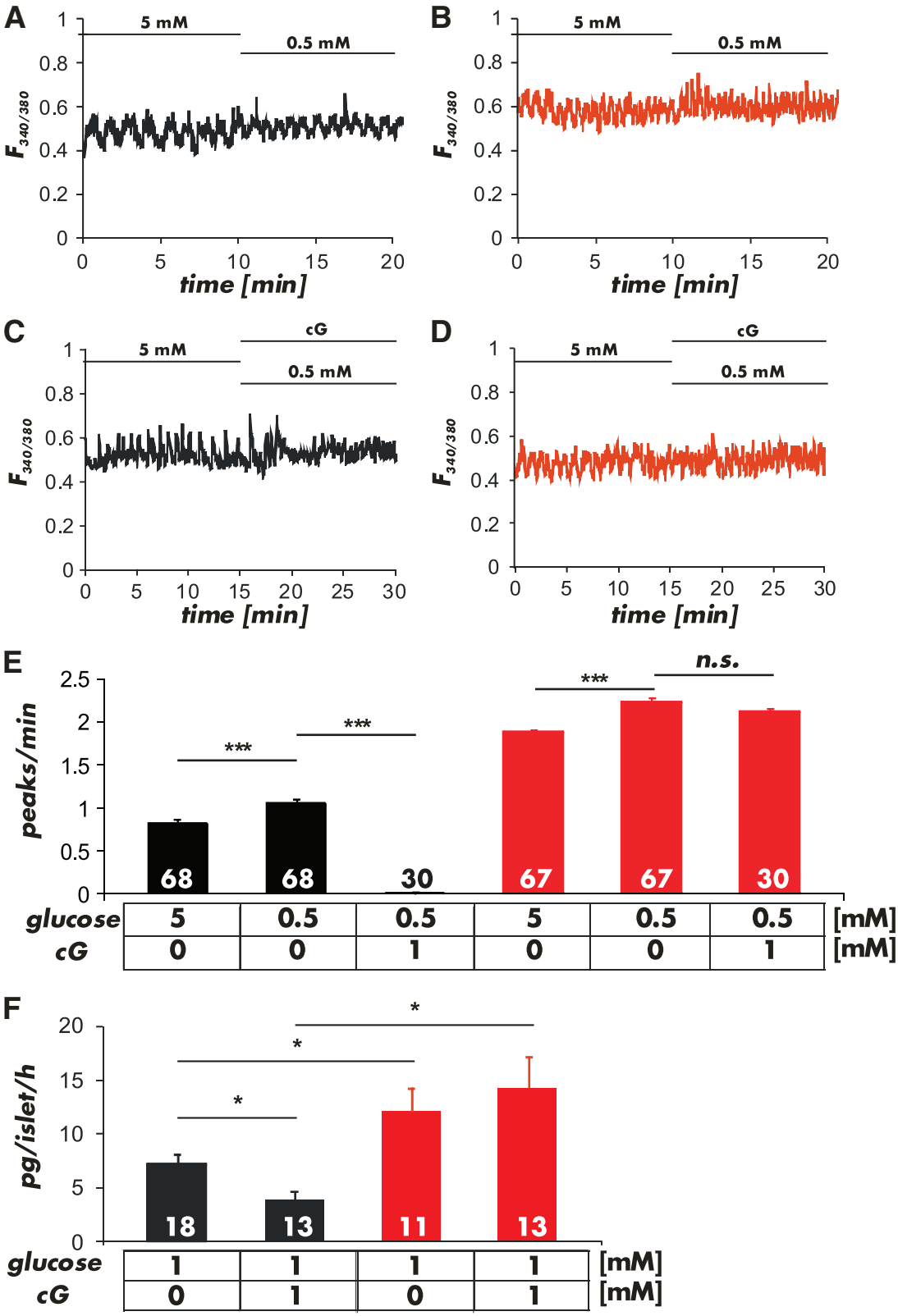

FIG. 6. Ca^{2+} transients of pancreatic α-cells measured in whole islets. *A* and *B*: Representative changes in FURA-2 fluorescence ratios at 5 mmol/l and 0.5 mmol/l glucose measured in control (*black*) and cGKI-KO (red) islets. *C* and *D*: Representative Ca^{2+}-transients measured in the presence or absence of 8-Br-cGMP (cG; 1 mmol/l) in control (*black*) and cGKI-KO (*red*) islets. *E*: Summary of the experiments shown in *A–D*. The frequency of Ca^{2+} oscillations at 5 mmol/l and 0.5 mmol/l glucose was significantly higher in cGKI-KO islets and was not reduced by the addition of 8-Br-cGMP (1 mmol/l). The numbers of cells that were measured under the particular conditions are given in the respective panels. Cells were from 14 CTR and 9 KO islets isolated from 5 CTR and 3 cGKI-KO mice, respectively. *F*: The release of glucagon was significantly increased in isolated cGKI-KO (ko) islets (*red bars*). 8-Br-cGMP (1 mmol/l) had no effect on the release rate of cGKI-KO islets, but suppressed glucagon release of control (ctr) islets (*black bars*) (*$P < 0.05$; ***$P < 0.001$). (A high-quality color representation of this figure is available in the online issue.)

8-Br-cGMP. Therefore, we measured the glucagon release in islets in the absence and presence of 8-Br-cGMP. Indeed, 8-Br-cGMP suppressed the release of glucagon in CTR islets from 7.19 ± 0.88 pg/islet/h (n = 18) to 3.85 ± 0.85 pg/islet/h (n = 13), whereas it had no effect on KO islets (12.13 ± 2.10 pg/islet/h [n = 11] and 14.36 ± 2.77 pg/islet/h [n = 13]) (Fig. 6*F*).

DISCUSSION

This manuscript provides novel genetic evidence for the presence of cGKIα in murine islets. We have shown that cGKIα has significant functional effects by the following main findings: *1*) cGKIα is expressed in glucagon secreting α-cells and in some SST-positive δ-cells of the Langerhans islet; *2*) active cGKI decreased glucagon secretion from islets at 1 mmol/l glucose; *3*) active cGKI suppressed calcium oscillation in α-cells at 0.5 mmol/l glucose; and *4*) serum glucose and glucagon levels were higher in the absence of islet cGKI than in CTR mice after 12-h fasting. In addition to cGKIα, we and others detected several components of the NO/cGMP and NP/cGMP pathways in mouse islets, including sGC, pGC, and PDE-5 (20,31). These findings establish cGKIα as an important signaling molecule that affects glucose metabolism in the mouse.

It has been shown that ANP inhibited glucagon and insulin release in isolated rat islets (39,40). Variable results for NO-donors and NOS inhibitors have been reported when used at low and high glucose concentrations (7,10). In line with our results, NO stimulated rat islet cGMP levels (14,41,42) and inhibited glucagon release most likely by a cGMP-induced decrease of $[Ca^{2+}]_i$ (43), supporting our observation that the endogenous cGKI suppresses $[Ca^{2+}]_i$ handling and glucagon release.

As recognized for many physiologic processes, such as vascular tone, platelet activation, and synaptic plasticity (22), our data indicate that cGKI interferes with the rise of $[Ca^{2+}]_i$, which is associated with glucagon secretion in α-cells. The molecular mechanism underlying the modulation of glucose-suppressed glucagon release by cGKI is unknown. Recently, it was implied that the activity of ATP-dependent K^+ (K_{ATP}) channels is modulated by recombinant cGKIα, leading to an increased open probability of the channel (44). K_{ATP}-channels have been proposed to play a key role in the regulation of α-cell electrical activity (45,46). According to this hypothesis, α-cell electrical activity (and thus glucagon secretion) is only possible in a narrow window of K_{ATP}-channel activity. Both increased (via membrane hyperpolarization and inhibition of action potential firing) and decreased K_{ATP}-channel (via membrane depolarization and voltage-dependent inactivation of the conductances involved in regenerative electrical activity) leads to suppression of glucagon secretion. However, the regulation of glucagon secretion is more complicated since it has been shown that exocytosis can as well be triggered by membrane depolarization via a voltage-dependent inactivation of ion channels involved in action potential generation (46). We cannot exclude the possibility that cGKI modulates Ca^{2+} influx (25,47) through voltage-dependent Ca^{2+}-channels (29,48) in the α-cells.

In addition to the findings summarized above, the gene-targeted cGKI mice showed an improved glucose clearance in the OGTT (see supplementary Fig. 2) that might be due to *1*) the small initial increase in serum insulin concentrations during the OGTT; *2*) a reduced body fat mass and FFA; *3*) the upregulation of GLUT4 in striated muscles, and *4*) the lack of cGKI in the central nervous system (49), which could impact islets innervations via, for example, sympathetic nerve fibers during the OGTT. Indeed, the importance of cGKI for the biogenesis of adipose tissue and fat accumulation was recently recognized (50). It is known that SST released from δ-cells and from extra-islet neuroendocrine cells exerts many relevant actions on islet physiology. Since small amounts of cGKI were present in δ-cells of CTR mice, but not in δ-cells of cGKI gene-targeted mice (see supplementary Fig. 3), an altered control of paracrine mechanisms from δ-cells has also been taken into account. Together, the lack of cGKI in the periphery and in δ-cells of gene-targeted mice might produce an inappropriate insulin response, which was noticed upon fasting when these animals were hyperglycemic (see Fig. 1).

In conclusion, the presented experiments identify α-cell cGKI as an endogenous modulator of the glucose-induced inhibition of glucagon release. The loss of islet cGKI activity in mice leads to an abnormal glucagon secretion, which is reflected by their hyperglycemic fasting phenotype.

ACKNOWLEDGMENTS

This work was supported by the Deutsche Forschungsgemeinschaft (FOR923) with grants to F.H. and R.L. and by the Research Funding Programme for Young Scientists at the University of Tübingen to R.L.

No potential conflicts of interest relevant to this article were reported.

V.L. performed research, analyzed data, and wrote the manuscript. A.F. contributed new tools, contributed to discussion, and reviewed/edited the manuscript. A.W. analyzed data, contributed to discussion, and reviewed/edited the manuscript. F.H. designed research, analyzed data, and wrote the manuscript. R.L. designed and performed research, analyzed data, and wrote the manuscript.

The authors thank Sabine Brummer (Institut für Pharmakologie und Toxikologie, TU München) and Teodora Kennel (DFG FOR923, TU München) for their excellent technical help. They acknowledge the support of Dominik ter Meer (TU München) at the Bioplex machine. They are grateful to Dr. Sergei Rybalkin (Department of Pharmacology, University of Washington, Seattle, Washington) for making the PDE-5 antibody available and to Dr. Peter Ruth (Institut für Pharmazie, Abteilung Pharmakologie, Toxikologie and Klinische Pharmazie, Universität Tübingen) for many helpful discussions.

REFERENCES

1. Gromada J, Franklin I, Wollheim CB. α-cells of the endocrine pancreas: 35 years of research but the enigma remains. Endocr Rev 2007;28:84–116
2. Leung YM, Ahmed I, Sheu L, Gao X, Hara M, Tsushima RG, Diamant NE, Gaisano HY. Insulin regulates islet α-cell function by reducing KATP channel sensitivity to adenosine 5′-triphosphate inhibition. Endocrinology 2006;147:2155–2162
3. Ravier MA, Rutter GA. Glucose or insulin, but not zinc ions, inhibit glucagon secretion from mouse pancreatic α-cells. Diabetes 2005;54:1789–1797
4. Rorsman P, Berggren PO, Bokvist K, Ericson H, Mohler H, Ostenson CG, Smith PA. Glucose-inhibition of glucagon secretion involves activation of GABAA-receptor chloride channels. Nature 1989;341:233–236
5. Gromada J, Hoy M, Buschard K, Salehi A, Rorsman P. Somatostatin inhibits exocytosis in rat pancreatic α-cells by G(i2)-dependent activation of calcineurin and depriming of secretory granules. J Physiol 2001;535:519–532

6. Vieira E, Salehi A, Gylfe E. Glucose inhibits glucagon secretion by a direct effect on mouse pancreatic α cells. Diabetologia 2007;50:370–379
7. Spinas GA, Laffranchi R, Francoys I, David I, Richter C, Reinecke M. The early phase of glucose-stimulated insulin secretion requires nitric oxide. Diabetologia 1998;41:292–299
8. Panagiotidis G, Alm P, Lundquist I. Inhibition of islet nitric oxide synthase increases arginine-induced insulin release. Eur J Pharmacol 1992;229:277–278
9. Alm P, Ekstrom P, Henningsson R, Lundquist I. Morphological evidence for the existence of nitric oxide and carbon monoxide pathways in the rat islets of Langerhans: an immunocytochemical and confocal microscopical study. Diabetologia 1999;42:978–986
10. Schmidt HH, Warner TD, Ishii K, Sheng H, Murad F. Insulin secretion from pancreatic B cells caused by L-arginine-derived nitrogen oxides. Science 1992;255:721–723
11. Salehi A, Carlberg M, Henningson R, Lundquist I. Islet constitutive nitric oxide synthase: biochemical determination and regulatory function. Am J Physiol 1996;270:C1634–C1641
12. Henningsson R, Salehi A, Lundquist I. Role of nitric oxide synthase isoforms in glucose-stimulated insulin release. Am J Physiol Cell Physiol 2002;283:C296–C304
13. Akesson B, Henningsson R, Salehi A, Lundquist I. Islet constitutive nitric oxide synthase and glucose regulation of insulin release in mice. J Endocrinol 1999;163:39–48
14. Jones PM, Persaud SJ, Bjaaland T, Pearson JD, Howell SL. Nitric oxide is not involved in the initiation of insulin secretion from rat islets of Langerhans. Diabetologia 1992;35:1020–1027
15. Corbett JA, Wang JL, Hughes JH, Wolf BA, Sweetland MA, Lancaster JR Jr, McDaniel ML. Nitric oxide and cyclic GMP formation induced by interleukin 1 β in islets of Langerhans. Evidence for an effector role of nitric oxide in islet dysfunction. Biochem J 1992;287(Pt 1):229–235
16. Burkart V, Kolb H. Nitric oxide in the immunopathogenesis of type 1 diabetes. Handb Exp Pharmacol 2000;143:525–544
17. Akesson B, Lundquist I. Influence of nitric oxide modulators on cholinergically stimulated hormone release from mouse islets. J Physiol 1999; 515(Pt 2):463–473
18. Hope KM, Tran PO, Zhou H, Oseid E, Leroy E, Robertson RP. Regulation of α-cell function by the β-cell in isolated human and rat islets deprived of glucose: the "switch-off" hypothesis. Diabetes 2004;53:1488–1495
19. Mergia E, Friebe A, Dangel O, Russwurm M, Koesling D. Spare guanylyl cyclase NO receptors ensure high NO sensitivity in the vascular system. J Clin Invest 2006;116:1731–1737
20. Laychock SG, Modica ME, Cavanaugh CT. L-arginine stimulates cyclic guanosine 3′,5′-monophosphate formation in rat islets of Langerhans and RINm5F insulinoma cells: evidence for L-arginine:nitric oxide synthase. Endocrinology 1991;129:3043–3052
21. Antoine MH, Hermann M, Herchuelz A, Lebrun P. Sodium nitroprusside inhibits glucose-induced insulin release by activating ATP-sensitive K+ channels. Biochim Biophys Acta 1993;1175:293–301
22. Hofmann F, Feil R, Kleppisch T, Schlossmann J. Function of cGMP-dependent protein kinases as revealed by gene deletion. Physiol Rev 2006;86:1–23
23. Pfeifer A, Klatt P, Massberg S, Ny L, Sausbier M, Hirneiss C, Wang GX, Korth M, Aszodi A, Andersson KE, Krombach F, Mayerhofer A, Ruth P, Fassler R, Hofmann F. Defective smooth muscle regulation in cGMP kinase I-deficient mice. Embo J 1998;17:3045–3051
24. Lukowski R, Rybalkin SD, Loga F, Leiss V, Beavo JA, Hofmann F. Cardiac hypertrophy is not amplified by deletion of cGMP-dependent protein kinase I in cardiomyocytes. Proc Natl Acad Sci U S A 2010;107:5646–5651
25. Weber S, Bernhard D, Lukowski R, Weinmeister P, Worner R, Wegener JW, Valtcheva N, Feil S, Schlossmann J, Hofmann F, Feil R. Rescue of cGMP kinase I knockout mice by smooth muscle specific expression of either isozyme. Circ Res 2007;101:1096–1103
26. Herrera PL. Adult insulin- and glucagon-producing cells differentiate from two independent cell lineages. Development 2000;127:2317–2322
27. Postic C, Shiota M, Niswender KD, Jetton TL, Chen Y, Moates JM, Shelton KD, Lindner J, Cherrington AD, Magnuson MA. Dual roles for glucokinase in glucose homeostasis as determined by liver and pancreatic β cell-specific gene knock-outs using Cre recombinase. J Biol Chem 1999;274: 305–315
28. Wegener JW, Nawrath H, Wolfsgruber W, Kuhbandner S, Werner C, Hofmann F, Feil R. cGMP-dependent protein kinase I mediates the negative inotropic effect of cGMP in the murine myocardium. Circ Res 2002;90:18–20
29. Vignali S, Leiss V, Karl R, Hofmann F, Welling A. Characterization of voltage-dependent sodium and calcium channels in mouse pancreatic A- and B-cells. J Physiol 2006;572:691–706
30. Geiselhoringer A, Gaisa M, Hofmann F, Schlossmann J. Distribution of IRAG and cGKI-isoforms in murine tissues. FEBS Lett 2004;575:19–22
31. Ropero AB, Soriano S, Tuduri E, Marroqui L, Tellez N, Gassner B, Juan-Pico P, Montanya E, Quesada I, Kuhn M, Nadal A. The atrial natriuretic peptide and guanylyl cyclase-A system modulates pancreatic β-cell function. Endocrinology. 2010;151:3665–3674
32. Lucas KA, Pitari GM, Kazerounian S, Ruiz-Stewart I, Park J, Schulz S, Chepenik KP, Waldman SA. Guanylyl cyclases and signaling by cyclic GMP. Pharmacol Rev 2000;52:375–414
33. Salehi A, Vieira E, Gylfe E. Paradoxical stimulation of glucagon secretion by high glucose concentrations. Diabetes 2006;55:2318–2323
34. Barg S. Mechanisms of exocytosis in insulin-secreting B-cells and glucagon-secreting A-cells. Pharmacol Toxicol 2003;92:3–13
35. Quoix N, Cheng-Xue R, Guiot Y, Herrera PL, Henquin JC, Gilon P. The GluCre-ROSA26EYFP mouse: a new model for easy identification of living pancreatic α-cells. FEBS Lett 2007;581:4235–4240
36. Wang JL, McDaniel ML. Secretagogue-induced oscillations of cytoplasmic Ca2+ in single β and α-cells obtained from pancreatic islets by fluorescence-activated cell sorting. Biochem Biophys Res Commun 1990;166:813–818
37. Olsen HL, Theander S, Bokvist K, Buschard K, Wollheim CB, Gromada J. Glucose stimulates glucagon release in single rat α-cells by mechanisms that mirror the stimulus-secretion coupling in β-cells. Endocrinology 2005;146:4861–4870
38. Le Marchand SJ, Piston DW. Glucose suppression of glucagon secretion: metabolic and calcium responses from α-cells in intact mouse pancreatic islets. J Biol Chem 2010;285:14389–14398
39. Verspohl EJ, Bernemann IK. Atrial natriuretic peptide (ANP)-induced inhibition of glucagon secretion: mechanism of action in isolated rat pancreatic islets. Peptides 1996;17:1023–1029
40. Ahren B. ANF inhibits glucose-stimulated insulin secretion in mouse and rat. Am J Physiol 1988;255:E579–E582
41. Green IC, Delaney CA, Cunningham JM, Karmiris V, Southern C. Interleukin-1 beta effects on cyclic GMP and cyclic AMP in cultured rat islets of Langerhans-arginine-dependence and relationship to insulin secretion. Diabetologia 1993;36:9–16
42. Panagiotidis G, Akesson B, Rydell EL, Lundquist I. Influence of nitric oxide synthase inhibition, nitric oxide and hydroperoxide on insulin release induced by various secretagogues. Br J Pharmacol 1995;114:289–296
43. Sugino F, Ishikawa T, Nakada S, Kaneko Y, Yamamoto Y, Nakayama K. Inhibition by nitric oxide of Ca(2+) responses in rat pancreatic α-cells. Life Sci 2002;71:81–89
44. Chai Y, Lin YF. Dual regulation of the ATP-sensitive potassium channel by activation of cGMP-dependent protein kinase. Pflugers Arch 2008;456:897–915
45. Gopel SO, Kanno T, Barg S, Weng XG, Gromada J, Rorsman P. Regulation of glucagon release in mouse cells by KATP channels and inactivation of TTX-sensitive Na+ channels. J Physiol 2000;528:509–520
46. MacDonald PE, De Marinis YZ, Ramracheya R, Salehi A, Ma X, Johnson PR, Cox R, Eliasson L, Rorsman P. A K ATP channel-dependent pathway within α cells regulates glucagon release from both rodent and human islets of Langerhans. PLoS Biol 2007;5:e143
47. Ropero AB, Soria B, Nadal A. A nonclassical estrogen membrane receptor triggers rapid differential actions in the endocrine pancreas. Mol Endocrinol 2002;16:497–505
48. Schulla V, Renstrom E, Feil R, Feil S, Franklin I, Gjinovci A, Jing XJ, Laux D, Lundquist I, Magnuson MA, Obermuller S, Olofsson CS, Salehi A, Wendt A, Klugbauer N, Wollheim CB, Rorsman P, Hofmann F. Impaired insulin secretion and glucose tolerance in β cell-selective Ca(v)1.2 Ca2+ channel null mice. Embo J 2003;22:3844–3854
49. Paul C, Schoberl F, Weinmeister P, Micale V, Wotjak CT, Hofmann F, Kleppisch T. Signaling through cGMP-dependent protein kinase I in the amygdala is critical for auditory-cued fear memory and long-term potentiation. J Neurosci 2008;28:14202–14212
50. Haas B, Mayer P, Jennissen K, Scholz D, Diaz MB, Bloch W, Herzig S, Fassler R, Pfeifer A. Protein kinase G controls brown fat cell differentiation and mitochondrial biogenesis. Sci Signal 2009;2:ra78.